

1    **Ventilation does not affect influenza virus transmission efficiency in a ferret playpen setup**

2

3    Authors: Nicole C. Rockey<sup>a,e</sup>, Valerie Le Sage<sup>a,1</sup>, Meredith Shephard<sup>b,1</sup>, Nahara Vargas-  
4    Maldonado<sup>b</sup>, Andrea J. French<sup>a</sup>, Sydney Walter<sup>a</sup>, Lucas M. Ferreri<sup>b</sup>, Katie E. Holmes<sup>b</sup>, David  
5    VanInsberghe<sup>b</sup>, Herek Clack<sup>c</sup>, Aaron J. Prussin II<sup>d</sup>, Anice C. Lowen<sup>b</sup>, Linsey C. Marr<sup>d</sup>, Seema S.  
6    Lakdawala<sup>a,b\*</sup>

7

8    <sup>a</sup>Department of Microbiology & Molecular Genetics, The University of Pittsburgh, Pittsburgh,  
9    PA 15219

10    <sup>b</sup>Department of Microbiology & Immunology, Emory University, Atlanta, GA 30322

11    <sup>c</sup>Department of Civil and Environmental Engineering, University of Michigan, Ann Arbor, MI  
12    48109

13    <sup>d</sup>Department of Civil and Environmental Engineering, Virginia Tech, Blacksburg, VA 24061

14

15    \*Corresponding author – Seema S. Lakdawala

16    1510 Clifton Rd, 3001 Rollins Research Center, Atlanta, GA 30322

17    Telephone: (404) 727-5950, Email: [seema.s.lakdawala@emory.edu](mailto:seema.s.lakdawala@emory.edu)

18

19    <sup>1</sup>Authors contributed equally.

20

21    Current affiliations:

22    <sup>e</sup>Department of Civil and Environmental Engineering, Duke University, Durham, NC 27708

23

24 **Abstract**

25 Sustained community spread of influenza viruses relies on efficient person-to-person  
26 transmission. Current experimental transmission systems do not mimic environmental conditions  
27 (e.g., air exchange rates, flow patterns), host behaviors or exposure durations relevant to real-  
28 world settings. Therefore, results from these traditional systems may not be representative of  
29 influenza virus transmission in humans. To address this pitfall, we developed a modified, more  
30 realistic transmission setup and used it to investigate the impact of ventilation rates on  
31 transmission in a close-range, play-based scenario. In this setup, four immunologically naïve  
32 recipient ferrets were exposed to a donor ferret infected with a genetically barcoded 2009 H1N1  
33 virus (H1N1pdm09) for four hours. The ferrets interacted in a shared space that included toys,  
34 similar to a child care setting. The transmission efficiency was determined under conditions of  
35 low and high ventilation rates; air exchange rates of  $\sim 1.3 \text{ hr}^{-1}$  and  $23 \text{ hr}^{-1}$ , respectively. Despite  
36 the large difference in ventilation rate, transmission efficiency was the same, 50% in two  
37 independent replicate studies. The presence of infectious virus or viral RNA on surfaces and in  
38 air throughout the exposure area was similar regardless of ventilation rate. While high viral  
39 genetic diversity in donor ferret nasal washes was maintained during infection, recipient ferret  
40 nasal washes displayed low diversity, revealing a narrow transmission bottleneck regardless of  
41 ventilation rate. Our findings indicate that in exposures characterized by frequent close-range,  
42 play-based interactions and the presence of fomites, ventilation does not significantly impact  
43 transmission efficiency.

44

45 **Significance**

46 Improved ventilation in building has the potential to reduce transmission of respiratory viruses,  
47 but its effect in different settings is not well understood. We developed a novel system to study  
48 influenza virus transmission in the ferret animal model in an environment that mimics a child  
49 care center. We demonstrate that increased ventilation is not effective at disrupting transmission  
50 in this setting, suggesting that transmission occurs mainly at close-range or via fomites. Multiple  
51 interventions are needed to reduce the spread of influenza virus in this type of setting.

52

### 53      **Introduction**

54           Seasonal and pandemic influenza viruses cause tens of thousands of deaths each year in  
55           the US (1). To circulate successfully in the human population, viruses must sustain human-to-  
56           human spread. Influenza virus transmission occurs via numerous routes, including direct and  
57           indirect (e.g., fomites) contact, inhalation of aerosols, and spray of large droplets (2–6). While all  
58           modes of transmission may occur during an exposure event, the relative contribution of each of  
59           these routes varies depending on host, environmental, and viral factors (3).

60           Certain settings are linked with elevated rates of transmission, including households and  
61           child care settings (7–10). In these situations, individuals interact in close proximity for extended  
62           periods of time (e.g., hours). Understanding how influenza virus transmission occurs and what  
63           interventions may reduce spread in these settings is critical, but conclusive data is lacking.

64           Randomized control trials and observational epidemiological studies in combination with  
65           modeling efforts have expanded knowledge in this area, and while some find marginal  
66           associations of hand hygiene and face mask use with lower levels of illness, most studies do not  
67           detect a statistical difference (11–19). Unfortunately, these studies have not decisively identified  
68           effective prevention strategies or predominant transmission routes because of confounding  
69           factors or limited adherence to interventions.

70           To fill this knowledge gap, controlled human transmission studies have been suggested  
71           (20). To date, two human influenza transmission studies have been conducted to mimic  
72           exposures in close living spaces (21, 22). The first proof-of-concept pilot resulted in transmission  
73           to three of 12 recipients (22), while the higher-powered study only observed transmission to one  
74           of 75 recipients (21). The expense of human challenge research and difficulties in consistently  
75           attaining influenza virus transmission have constrained this work.

76 More commonly, animal models of influenza virus transmission, and in particular the  
77 ferret model, are used to assess transmission dynamics of influenza viruses (23). Results of prior  
78 studies may not be representative of transmission in real-world contexts since the experimental  
79 setups typically use directional airflow, elevated ventilation, lengthy exposure durations, and/or  
80 restricted donor-to-recipient interactions (24–32). While some studies have used shortened  
81 exposure durations to shift towards more realistic transmission systems (33, 34), a number of  
82 features still do not recapitulate everyday interactions among humans.

83 To reduce respiratory virus spread in high-risk settings, non-pharmaceutical interventions  
84 are often recommended (35, 36). Common environmental controls include barriers, physical  
85 distancing, masking, filtration, ventilation, and humidification. These strategies aim to decrease  
86 exposure to infectious virus in the air. Increasing ventilation, which reduces concentrations of  
87 contaminants in air and subsequent deposition of virus on surfaces, has been suggested to reduce  
88 influenza virus transmission rates (37–41). However, these studies contain significant  
89 limitations: modeling components rely on unvalidated assumptions and observational studies  
90 often include uncontrolled variables such that causality cannot be firmly established. Thus, an  
91 experimental setting that mimics real-world transmission scenarios is critical for studying how  
92 viruses transmit and assessing the impact of recommended engineering controls, such as  
93 ventilation, on virus spread.

94 Transmission to a new host often vastly changes the genetic composition of a viral  
95 population. This effect has important implications for viral evolution and can potentially also  
96 offer insight into the physical and biological processes that shape the transmission event.-Indeed,  
97 previous animal studies evaluating transmission bottlenecks provided evidence that the route of  
98 infection influences the diversity transferred between hosts (42, 43). Nevertheless, it remains

99 unclear how environmental conditions and host behavior impact the transfer of viral diversity  
100 between hosts during a transmission event.

101 In this study, we describe a novel exposure environment for studying influenza virus  
102 transmission among ferrets that more accurately recapitulates transmission in a scenario  
103 involving frequent close-range interactions among humans over several hours, such as those  
104 observed in child care settings. This system was used to assess how ventilation affects  
105 environmental contamination and transmission in play-based exposures. To increase the  
106 resolution of viral detection in recipient ferrets, we used a barcoded virus population. Our results  
107 indicate that, in a play-based scenario, increasing ventilation by a factor of 18 does not affect  
108 transmission efficiency or the number of distinct viral variants that establish infection. This work  
109 has important implications for informing the value of engineering controls in indoor  
110 environments. Our findings also highlight the role that exposure setting and associated behaviors  
111 may play in driving transmission, even in the presence of engineering controls like ventilation.

112 **Results**

113 ***Play-based system to study influenza virus transmission in ferrets.*** To examine  
114 influenza virus transmission efficiency in a more realistic setting, we developed a new ferret  
115 model system that allows for environmental conditions and behavior like those in a child care  
116 setting. Children in daycare facilities exhibit a wide range of behaviors and interactions,  
117 including close interactions with one another (e.g., touching, hugging) and exploratory behaviors  
118 involving touching and sharing toys or other objects. To simulate a child care setting under  
119 controlled experimental conditions, we used ferrets because their behaviors recapitulate many of  
120 those exhibited by children. Ferrets are curious animals that explore and play with toys and other

121 surfaces through touch and bite behavior. They are also social animals and display considerable  
122 close-range behaviors, including chasing, biting, nuzzling, and cuddling (44).

123 In our ferret transmission setup, recipient ferrets were housed with a single infected donor  
124 ferret in a defined area ( $\sim 3.5 \text{ m}^2$ ) for a single exposure period (see Fig.1, Methods, Movie S1,  
125 and Movie S2 for more details). This system allows for all modes of transmission: contact  
126 (including from toys and other objects), aerosol, and droplet spray. In each transmission  
127 experiment (Fig. 1A), the donor ferret was intranasally infected with  $10^6 \text{ TCID}_{50}$  of barcoded  
128 H1Npdm09 virus, placed in the exposure area at one day post-infection and allowed to interact  
129 with four naïve recipient ferrets for four continuous hours. Following the exposure period, all  
130 ferrets were individually housed. Nasal washes and oral swabs were collected to evaluate viral  
131 shedding and seroconversion of the recipients was determined on days 14 and 21 post donor  
132 infection (Fig. 1A).

133 Our system enabled us to modulate ventilation conditions to a low air exchange rate of  
134  $\sim 1.3$  air changes per hour, representative of those found in schools and child care facilities (45,  
135 46), or a high rate of  $\sim 23$  air changes per hour (Fig. 1B, Movies S1 and S2), exceeding  
136 ventilation rates that are recommended for healthcare facilities (47). This allowed us to assess the  
137 impact of elevated ventilation rate on transmission. The low ventilation condition was achieved  
138 by enclosing the transmission system within a tent. The air exchange rate in the tent was  
139 experimentally confirmed using the  $\text{CO}_2$  decay method (see Methods, Fig. S1). The elevated  
140 ventilation condition was attained by removing the tent. In this case, the air exchange rate was  
141 equal to that of the room in the animal facility and was calculated based on mechanical  
142 ventilation parameters (see Methods). Two independent transmission studies were performed for  
143 each ventilation condition.

144 For each transmission experiment, toys, food, and water were placed throughout the  
145 space to encourage ferret-object interactions (Fig. 1C). Additionally, several different types of  
146 aerosol collection devices, namely National Institute for Occupational Safety and Health  
147 (NIOSH) bioaerosol cyclone samplers, gelatin cassette samplers, and liquid Spot samplers, were  
148 placed within the exposure space to measure aerosolized infectious virus and viral RNA (Fig.  
149 2A). To assess fomite contamination, toys and other surfaces were swabbed post-exposure for  
150 infectious virus and viral RNA. CO<sub>2</sub> levels, which are indicative of exhaled breath, were  
151 measured using Aranet4 sensors and were higher in the low ventilation condition, as expected  
152 (Fig. S2). These sensors were also used to monitor relative humidity and temperature at different  
153 locations within the exposure area (Fig. S3). A remote-controlled battery-powered robot  
154 collected aerosols at close-range to the animals using NIOSH bioaerosol cyclone samplers and a  
155 gelatin cassette sampler; an Aranet4 sensor housed within the robot measured humidity,  
156 temperature, and CO<sub>2</sub> (Fig. 1C and Fig. 2A).

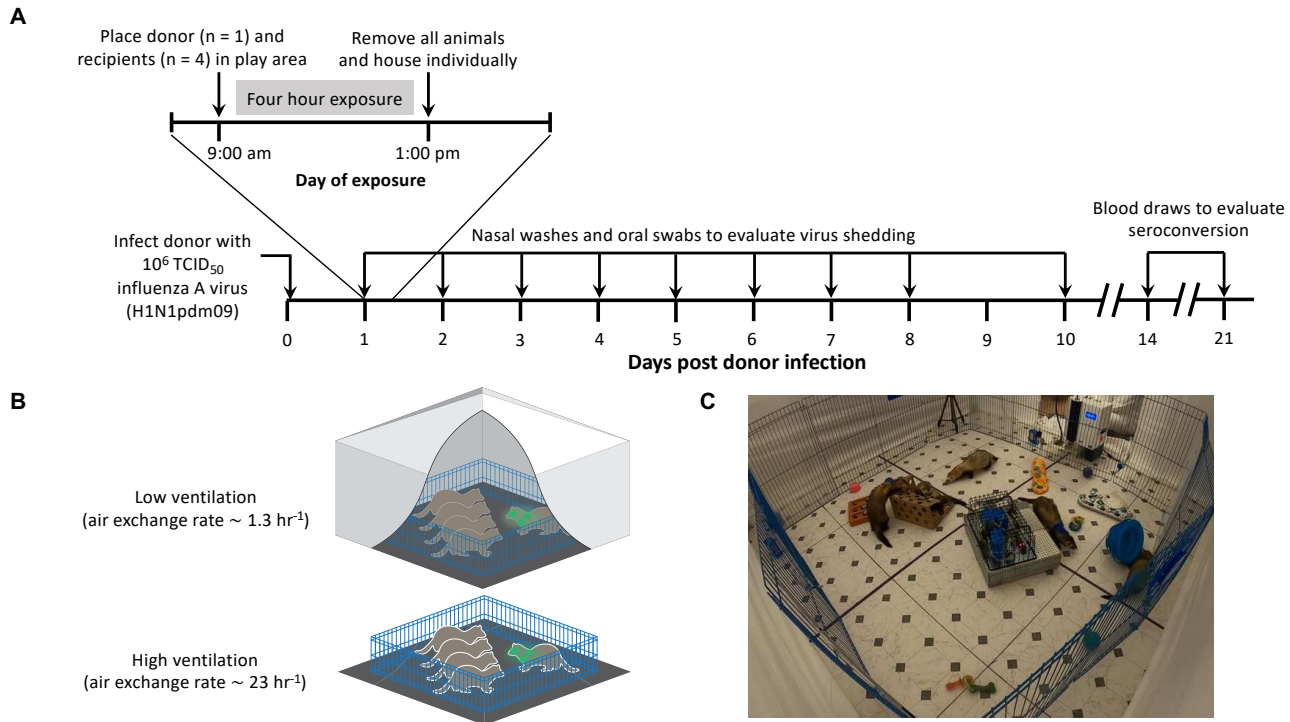


**Figure 1. Overview of the close-contact, play-based ferret transmission setup. (A)** Timeline of activities associated with the transmission experiments, (B) schematics of the transmission system for low and high ventilation settings, and (C) image of a transmission exposure experiment.

157        ***Viral RNA concentrations were not significantly lower when ventilation was increased.***

158        Ventilation is expected to reduce the concentrations of virus-containing aerosols within a space.

159        To assess the impact of ventilation on influenza virus-containing aerosols, we compared the

160        concentration of viral RNA in air from exposures with low and high ventilation rates (Fig. 2A).

161        We did not detect infectious virus in samples collected from any of three air-sampling devices

162        (data not shown), namely a Spot Sampler condensation particle collector, a NIOSH bioaerosol

163        cyclone sampler, and a gelatin cassette sampler, even though infectious virus was detected from

164        donor ferret aerosol expulsions sampled directly into the Spot Sampler (Fig. S4 and Methods).

165        Although no infectious influenza virus was detected from the air in the experimental enclosure,

166        viral RNA was captured using the NIOSH bioaerosol cyclone samplers in both the low and high

167 ventilation settings (Fig. 2B). No viral RNA was detected from the gelatin cassette or Spot  
168 Sampler (data not shown). The proportion of positive aerosol samples and the concentrations of  
169 viral RNA detected were not significantly different between the low and high ventilation  
170 experiments. Across two independent experiments, 50% (5/10) of samplers were positive in the  
171 high ventilation setting, while 70% (7/10) of samplers were positive in the low ventilation  
172 setting. Concentrations of viral RNA sampled using the NIOSH bioaerosol cyclone samplers in  
173 the high ventilation experiment were slightly lower, on average  $2.3 \log_{10}$  gene copies/L air, than  
174 in the low ventilation experiment, at  $2.5 \log_{10}$  gene copies/L air, although this difference was not  
175 significant (Mann-Whitney test,  $p = 0.31$ ). Therefore, increased ventilation did not appear to  
176 affect the amount of viral RNA in air sampled around the ferrets during the exposure period.

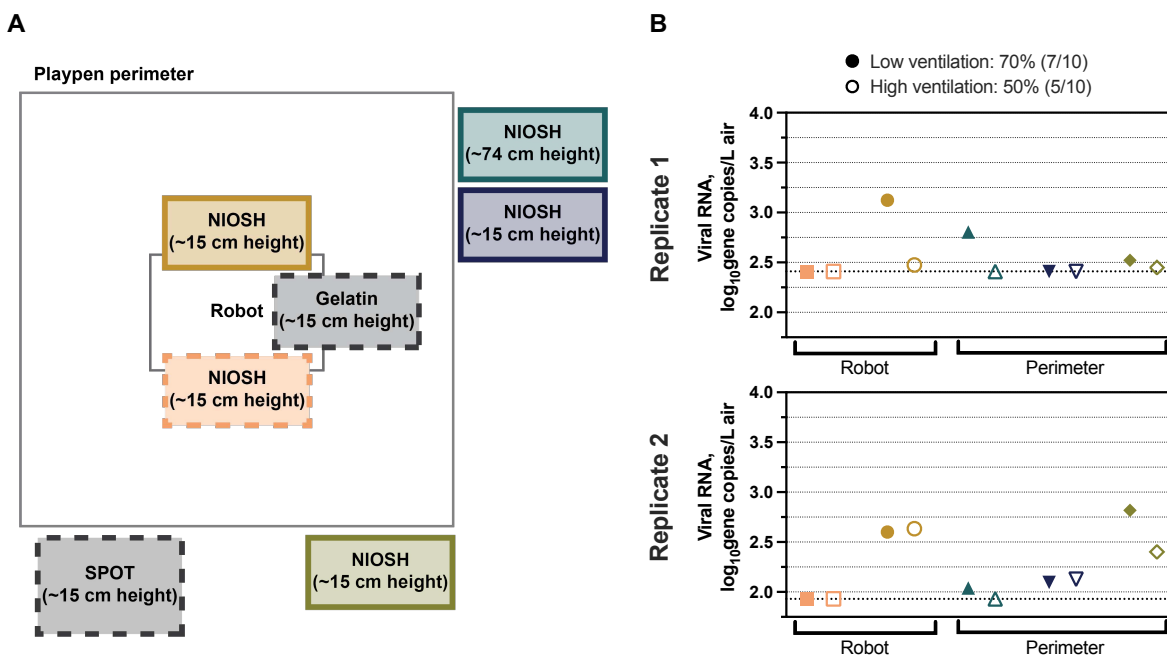


**Figure 2. Ventilation setting did not significantly impact viral RNA concentrations detected in aerosols. (A)** Schematic of air sampler locations, including the Spot Sampler aerosol particle collector (SPOT), gelatin cassette sampler (Gelatin), and NIOSH bioaerosol cyclone samplers (NIOSH). Dashed

outlines indicate samplers used to detect both infectious virus and viral RNA, and solid outlines indicate samplers used to detect only viral RNA. (B) Total influenza virus RNA concentrations collected from each NIOSH bioaerosol cyclone sampler during two independent experiments with low (closed symbols) or high (open symbols) ventilation. All three size fractions of the NIOSH bioaerosol cyclone sampler were analyzed for presence of viral RNA separately, but are shown here as the sum of all fractions. The color of symbols in (B) correspond to the NIOSH bioaerosol cyclone sampler shown in (A). Dashed lines indicate the limit of detection. NIOSH samplers, SPOT sampler, and gelatin cassette sampler were each run for the entire four-hour exposure at flow rates of 3.5, 1.4, and 1.5 L/min, respectively. No infectious virus was detected from any air samplers, and no viral RNA was detected in the gelatin cassette or Spot Sampler.

177                   *Surfaces in the transmission enclosures contained infectious virus, regardless of*  
178                   *ventilation rate.* Our transmission setup also provided the opportunity for ferrets to interact with  
179                   various toys and objects, similar to what may occur in a child care setting. Given the potential for  
180                   influenza virus shedding and subsequent contamination of fomites during each exposure, we  
181                   sampled surfaces and assessed the distribution and concentration of both infectious influenza  
182                   virus and viral RNA (Fig. 3A). The proportion of surface samples positive for infectious  
183                   influenza virus was the same across both replicate sets of experiments, with surface positivity in  
184                   13.5% of samples (7/52) in either ventilation setting (Fig. 3B). Concentrations were statistically  
185                   similar across the distinct ventilation settings (Mann-Whitney test,  $p = 0.88$ ), with a mean of 0.61  
186                    $\log_{10}$  TCID<sub>50</sub>/swab in the low ventilation setting and 0.62  $\log_{10}$  TCID<sub>50</sub>/swab in the high  
187                   ventilation setting.

188                   Detection of viral RNA on surfaces followed the same trend as that of infectious virus,  
189                   yielding similar concentrations across the low and high ventilation experiments (Mann-Whitney  
190                   test,  $p = 0.09$ ; low ventilation mean = 4.9  $\log_{10}$  gene copies/swab, high ventilation mean = 5.1

191  $\log_{10}$  gene copies/swab; Fig. 3C). As expected, viral RNA positivity was higher than infectious  
192 virus positivity, with 33% (17/52) and 44% (23/52) of surface samples being positive for viral  
193 RNA in the low and high ventilation exposures, respectively. Together, these results provide  
194 evidence that ventilation did not significantly impact the extent of surface contamination that  
195 occurred due to viral shedding from an infected ferret.

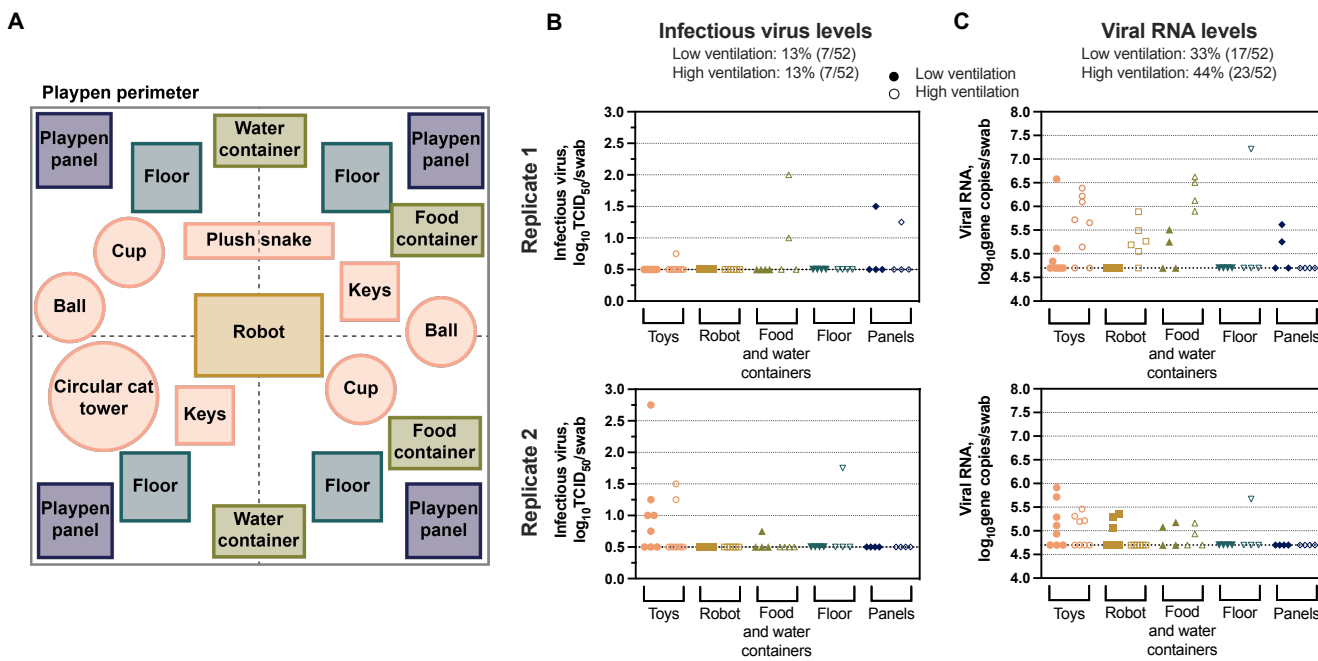


**Figure 3. Similar influenza virus concentrations from surfaces sampled following low and high ventilation transmission exposures.** (A) Schematic of all surfaces sampled following each transmission exposure. (B) Amount of infectious influenza virus detected on each surface grouped by object type for both replicates. (C) Total concentration of viral RNA per swab detected from surface samples group by object type during two independent experiments with low (closed symbols) or high (open symbols) ventilation. The color of symbols in (B) and (C) correspond to the samples of the same color shown in (A). Dashed lines indicate the limit of detection.

196 ***Increased ventilation did not reduce transmission in a play-based setting.*** Ultimately,  
197 we developed this transmission system to directly evaluate whether ventilation would affect the

198 efficiency of influenza virus spread in a play-based setting. In both low and high ventilation  
199 settings, four of eight (50%) of recipients shed virus beginning at least one day post-exposure  
200 (Fig. 4, Fig. S5). Seroconversion of recipient ferrets post-exposure confirmed these findings  
201 (Table S1). Of note, the onset of viral shedding in the nasal washes of infected recipients from  
202 the high ventilation setting was delayed by at least 24 hours compared to the viral shedding of  
203 infected recipients from the low ventilation setting. Virus loads in oral swabs followed the same  
204 overall trend, although the delay in onset was more subtle compared to nasal washes (Fig. S5).  
205 Clinical signs in the high ventilation and low ventilation groups were similar in infected  
206 recipients (Fig. S6). Together, our data suggest that in play-based settings with frequent  
207 interactions at close-range and multiple transmission modes likely at play, ventilation may not be  
208 effective in mitigating influenza virus spread.

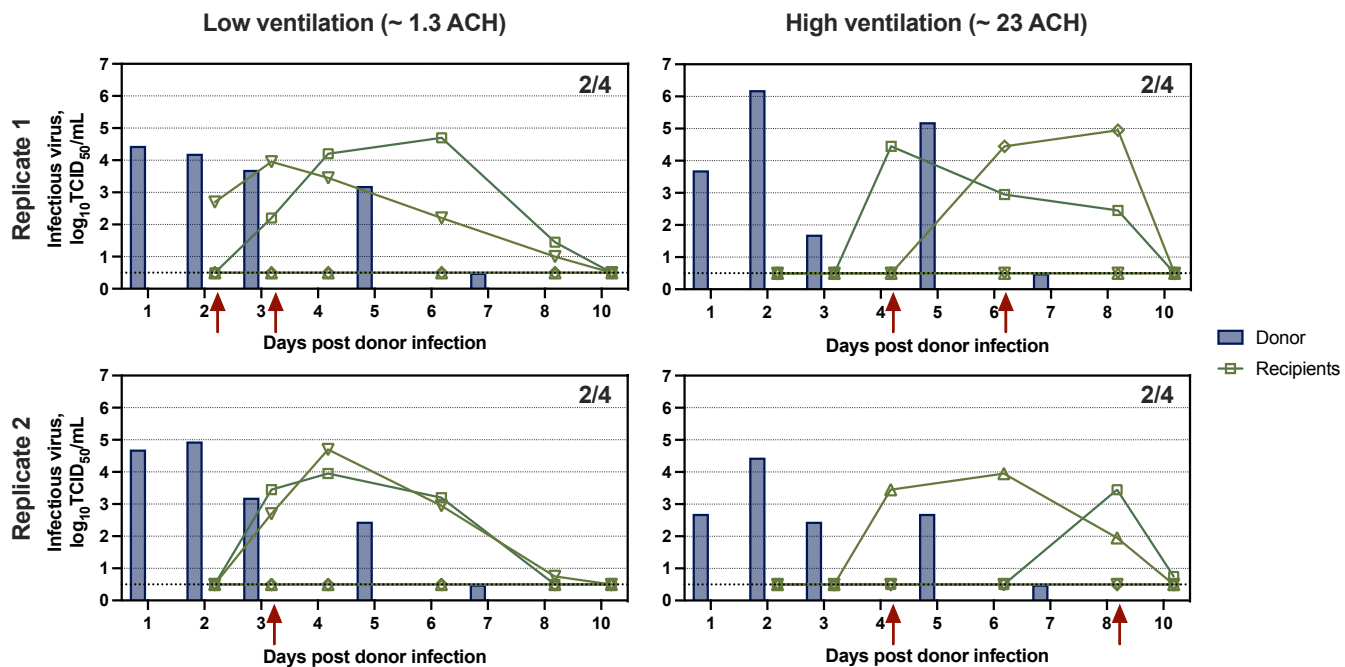


**Figure 4. Infectious influenza virus transmission and shedding kinetics in the nasal washes of donor and recipient ferrets under low and high ventilation exposure settings.** The transmission exposure

occurred the day after inoculation of donors, as indicated in Figure 1A. Dashed lines indicate the limit of detection. Fractions denote the amount of transmission that occurred in each experiment as determined by shedding and seroconversion. Red arrows indicate the days when virus shedding was first detected in nasal washes of recipient ferrets. Donor ferret nasal washes were collected on days 1, 2, 3, 5, and 7 post-infection, and recipient ferret nasal washes were collected on days 2, 3, 4, 6, 8, and 10 post donor-infection. ACH = air changes per hour.

209                    ***There is a narrow transmission bottleneck during play-based exposures regardless of***

210                    ***ventilation rate.*** Use of a barcoded virus library enables analysis of not only whether or not  
211                    transmission occurred, but also how many unique viral genomes established infection in the new  
212                    host. The barcoded H1N1pdm09 virus has twelve naturally occurring, bi-allelic sites resulting in  
213                    4096 unique viral genotypes designed to have equivalent fitness (Fig. S7 and Methods). At 24  
214                    hours post-inoculation, nasal washes from donor ferrets exhibited a high amount of viral  
215                    diversity, evidenced by the detection of > 3,000 barcodes at similar frequencies (Fig. 5). Barcode  
216                    diversity was maintained at a high level throughout the donor's infection (Fig. 5). In contrast, the  
217                    nasal washes of all recipient ferrets that became infected exhibited low barcode diversity, with  
218                    only one to three prominent barcodes detected in nasal washes (Fig. 5). This narrow bottleneck  
219                    occurred across both low and high ventilation conditions. Importantly, unique viral barcodes  
220                    were not repeated across recipients, as expected for fitness neutral genetic variants. These data  
221                    indicate that ventilation does not appear to impact the viral transmission bottleneck that occurs in  
222                    the play-based setting.

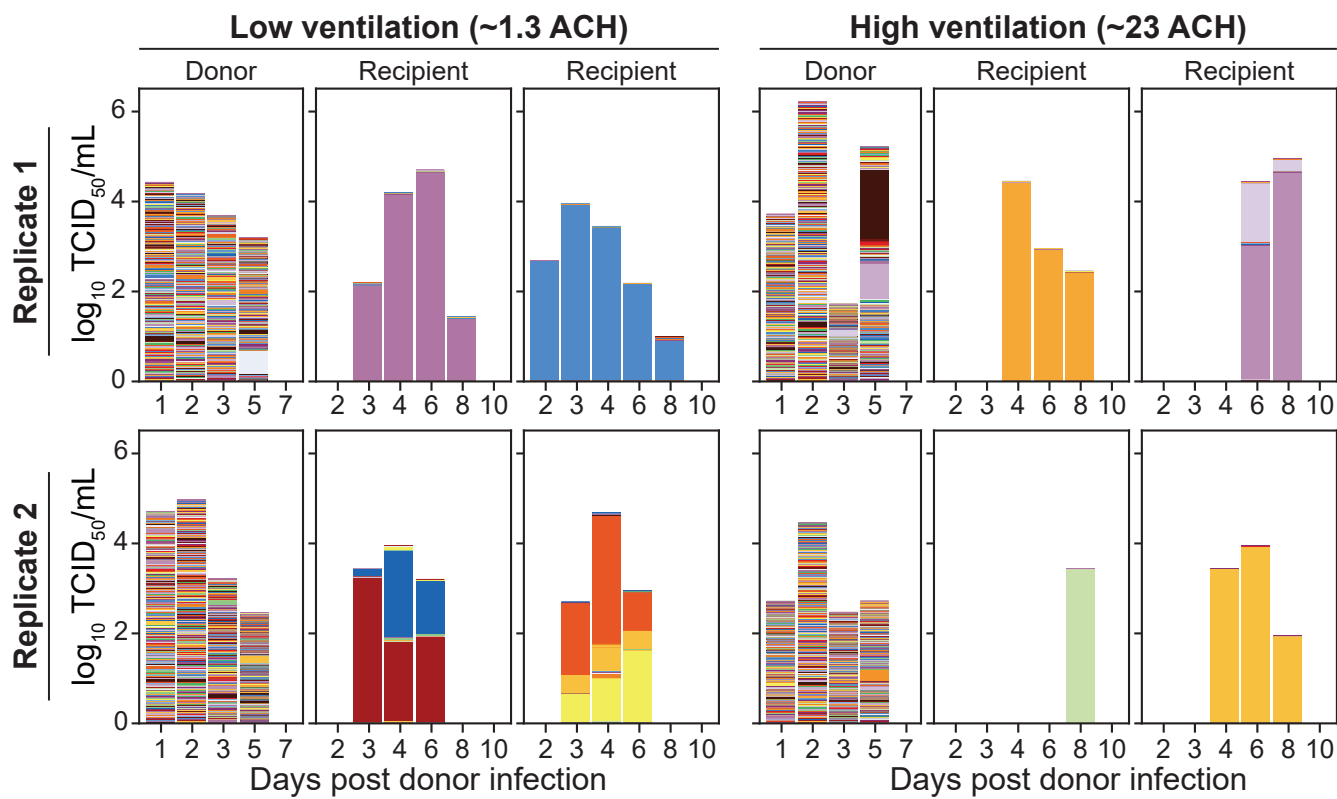


**Figure 5. Barcode dynamics in donor and recipient ferrets do not differ according to ventilation conditions.** The height of the bars represents viral titer on a log scale and the colors within each bar show the frequency of individual barcodes within the sample. Samples that had a  $\geq 1 \log_{10} \text{TCID}_{50}/\text{mL}$  were analyzed by next-generation sequencing. Each of the 4096 unique barcodes is displayed with a consistent color among all samples. None of the barcodes were shared between recipient ferrets in a singular experiment at frequencies  $> 1\%$ , emphasizing the neutrality of the barcode system. ACH = air changes per hour.

223

224 **Discussion**

225 While the ferret model has been the standard for studying influenza virus transmission  
226 dynamics, previous experiments have depended on particular cage configurations to force certain  
227 modes of transmission (e.g., airborne using perforated cage divider, all modes by co-housing)

228 and have employed elements (e.g., > 48 hr exposures, directional air flow) (23) that do not reflect  
229 the conditions under which humans are typically exposed. Our novel setup aims to simulate more  
230 realistic scenarios involving close-range interactions and play, such as those that might occur in a  
231 child care setting. This system allows us the opportunity to determine how interventions alter  
232 influenza virus spread in a setting with behaviors or interactions that lead to multiple modes of  
233 transmission. Here, we focused on ventilation, but future work can build on this system to  
234 evaluate whether other engineering controls, such as humidification, directional air flow,  
235 filtration, or antiviral coatings on surfaces may more effectively reduce transmission in close-  
236 contact scenarios.

237 Using this modified ferret model, we provide experimental evidence indicating that  
238 ventilation in play-based scenarios with frequent interactions at close-range, including with  
239 fomites, does not alter transmission efficiency of influenza virus. While many other influenza  
240 virus ferret studies use transmission systems with distinct ventilation rates, the direct study of  
241 how ventilation influences transmission in the ferret model has not been conducted to date (48).

242 A recent study with guinea pigs found that transmission efficiency was not affected by  
243 ventilation airflow speed, and the authors suggested that aerosolized virus resuspended from  
244 surfaces played a role in transmission (49). Previous work has drawn correlations between  
245 ventilation levels and observed human transmission rates (37, 50), but these studies were not  
246 designed to directly assess transmission efficiency derived from ventilation differences.

247 The effectiveness of an environmental intervention depends not only on the pathogen but  
248 also on host factors. The behavior modeled in this experiment is closer to that of children in a  
249 child care setting than adults in a workplace. The anatomy and stature of ferrets may contribute  
250 to enhanced loss of exhaled respiratory particles by gravitational settling and reduced potential

251 for them to disperse and be removed by ventilation. A 5  $\mu\text{m}$  particle released from a ferret's nose  
252 height, say 5 cm, will settle to the floor in about 1 minute, in contrast to > 20 minutes if released  
253 from a young child's mouth at a height of 100 cm. As acknowledged by the American Society of  
254 Heating, Refrigerating and Air-Conditioning Engineers' (ASHRAE) Standard 241 for control of  
255 infectious aerosols, ventilation has limited effectiveness for reducing the risk of transmission in  
256 close-range interactions and should be considered as one part of a multi-layered strategy (51). In  
257 settings where fewer close-range interactions occur, such as in a school with older children who  
258 remain seated at separate desks, office building, or retail store, increasing ventilation could still  
259 prove useful in limiting virus transmission.

260 Our results lend insight to where and how influenza virus transmission may be occurring  
261 in settings with close-range interactions. Transmission by direct contact was certainly possible.  
262 Environmental sampling provided evidence of influenza virus in aerosols and on surfaces,  
263 signifying that both short-range aerosol and indirect contact transmission could be occurring.  
264 Surface contamination was similar in both ventilation scenarios, while only slightly less viral  
265 RNA was noted in aerosols under increased ventilation. These aerosol viral RNA loads were not  
266 as different as would have been expected given the large change in ventilation rate, perhaps due  
267 to respiratory particles being removed by gravitational settling, as mentioned above. Most likely,  
268 virus concentrations were highest in the immediate vicinity of the ferrets, within a certain radius  
269 and low to the ground. Regardless of the underlying reason, NIOSH bioaerosol sampler  
270 placement at heights and locations accessible to infected ferrets were meant to represent aerosol  
271 exposures likely experienced by recipient ferrets, which ventilation only marginally affected in  
272 this study. Additional air samplers may be necessary in future studies to assess how virus-laden  
273 aerosols distribute depending on airflow. The modest reduction in viral RNA-containing aerosols

274 in the immediate vicinity of the ferrets was likely insufficient to disrupt transmission by an  
275 aerosol route. In addition, transmission by other modes would not be affected by ventilation.

276 We hypothesized that the low ventilation setting would result in greater viral barcode  
277 diversity in recipient nasal washes compared to the high ventilation setting. Contrary to this  
278 expectation, the viral populations that established in recipients from both ventilation conditions  
279 comprised few barcodes, indicating that ventilation had no major impact on the size of the  
280 transmission bottleneck in our system. The observed narrow genetic bottleneck aligns with  
281 previous work showing that only a limited number of genotypes establish sustained infection in a  
282 recipient (42, 43). These studies showed that, compared to transmission solely through the air,  
283 transmission between animals in direct contact yielded a looser genetic bottleneck. While our  
284 playpen system is more similar to the direct contact model, the brief exposure times we  
285 employed could explain the observed strong constriction in population diversity seen even at low  
286 ventilation and with all modes of transmission possible.

287 Although transmission efficiency was not affected by ventilation rate, shedding kinetics  
288 in nasal washes and oral swabs differed. The observed delays in shedding under high ventilation  
289 could be due to differences in infectious dose or anatomical site of viral deposition. While  
290 preliminary, these findings suggest that different settings or implementation of engineering  
291 controls might affect incubation time in situations with close interactions, thus impacting the  
292 timing of peak potential for onward transmission. In turn, these effects would carry implications  
293 for contact tracing and epidemiological modeling of transmission outbreaks.

294 There are limitations to the current study. Collection of infectious virus in aerosols from  
295 the experimental enclosures during transmission exposures proved difficult despite using three  
296 distinct sampling approaches. This outcome aligns with other work, which has also failed to

297 culture influenza virus from aerosols (52, 53), potentially due to dilute aerosol concentrations or  
298 harsh sampling techniques. Due to our lack of detection of infectious virus in aerosols, the fate of  
299 infectious virus from expelled aerosols under either low or high ventilation remains unclear.  
300 Future studies could consider raising sampling flow rates to overcome these technical challenges,  
301 although care must be taken to ensure aerosols sampling approaches are not so harsh as to  
302 inactivate virus. High flow rates could also increase the effective air exchange rate and affect the  
303 spatial distribution of virus in the space. Additionally, while ferrets are a valuable model for  
304 studying influenza virus transmission, these animals will never perfectly emulate humans. Ferret  
305 behavior may loosely resemble that of small children, but there are critical differences, including  
306 the prolonged contact napping of ferrets, as well as extensive biting or chewing, communal  
307 eating or drinking, and a lack of vocalization. Detailed analysis of ferret behaviors used during  
308 the play-based exposures will shed light on the activities associated with successful influenza  
309 virus transmission. Ultimately, human challenge studies or controlled observational  
310 epidemiology will be needed to ascertain whether the trends exhibited in this study can be  
311 recapitulated among humans. Nonetheless, this work is important to inform real-world settings,  
312 and is a critical first step to better characterizing transmission dynamics and evaluating  
313 engineering controls in close-contact scenarios where multiple modes of transmission may be  
314 operational.  
315

316 **Materials and Methods**

317 ***Influenza virus barcoded plasmid generation.*** The region of the influenza  
318 A/California/07/2009 (H1N1pdm09) genome used for barcode introduction was identified by  
319 aligning publicly available sequences of H1N1 viruses circulating in humans. A region with  
320 multiple synonymous nucleotide changes was identified from nucleotide position 429 to 489.  
321 These naturally occurring mutations were used to build synthetic diversity into the viral stock,  
322 thus avoiding the need to introduce foreign sequence into the viral genome (which typically  
323 attenuates replication) and limiting the potential for fitness differences among barcoded variants  
324 (which would result in their biased replication). Double-stranded Ultramers (IDT) were designed  
325 containing degenerate bases with two possible nucleotides at each of the twelve selected barcode  
326 sites (Forward: 5' –  
327 GACTCAAGGGGCCTGCTAAATGACAARCATTCTMAATGGRACCATWAARGACAGR  
328 AGYCCWTATCGRACYCTAATGAGCTGTCCYATWGGTGAAGTTCCCTCTCCATACAA  
329 CTCAAG – 3'; Reverse: 5' –  
330 CTTGAGTTGTATGGAGAGGAACTTCACCWATRGGACAGCTCATTAGRGTYCGATA  
331 WGGRCTYCTGTCYTTWATGGTYCCATTKGAAATGYTTGTCATTAGCAAGGCCCTTG  
332 AGTC – 3'). Carry-over of the NA wild-type sequence was limited by the addition of two stop  
333 codons within the barcode region of wild-type plasmid prior to insertion of ultramer DNA.  
334 Proper insertion of the ultramers removes the stop codons. Additionally, BarcodeID, our  
335 amplicon sequencing analysis software, described below, excludes reads that carry high quality  
336 bases that do not match the expected barcode sites. This feature leads to exclusion of any wild-  
337 type sequences containing the stop codons from downstream analyses.

338 Plasmid manipulation for barcode insertion was done as described in Holmes et al. (54),  
339 with the exception that the starting material used was the plasmid pHW Cal/07 NA (a kind gift of  
340 Dr. Jesse Bloom). Briefly, site-directed mutagenesis was used to introduce an Xho1 site within  
341 the wild-type barcode region within the NA segment. Next, the plasmid was linearized with  
342 Xho1 digestion, dephosphorylated using rSAP (NEB, Cat No. R0146L), and amplified by PCR  
343 using primers that extend outward from the extremes of barcode region (Forward: 5' –  
344 GTGAAGTTCCCTCTCCATACAACTCAAGATTGAG – 3'; Reverse: 5' –  
345 CTTGACTCAAGGGGCCTTGCTAAATGAC – 3'). This was followed by PCR purification  
346 using the QIAquick PCR Purification Kit (Qiagen, Cat. No. 28106) and elimination of residual  
347 wild-type sequences by enzymatic digestion with DPN1 and Xho1. A second PCR purification  
348 was performed prior to insertion of the Ultramers into the vector by DNA assembly with the  
349 NEBuilder HiFi DNA Assembly Kit (NEB, Cat. No. E2621). Next, the product was transformed  
350 into DH5- $\alpha$  cells (NEB, Cat. No. C2987H). Following culture on LB-ampicillin plates  
351 (Invitrogen, Cat. No. 45-0034), bacterial colonies were pooled into LB-ampicillin culture media  
352 and amplified followed by plasmid purification with the Plasmid Maxi Kit (Qiagen, Cat. No.  
353 12165). Barcode diversity in the plasmid stock was confirmed via next-generation sequencing  
354 (Amplicon-EZ – Azena Life Sciences). The diverse plasmid stock was then used to generate a  
355 barcoded H1N1pdm09 virus via reverse genetics by combining it with seven H1N1pdm09 wild-  
356 type gene segments encoded in pHW vectors (55).

357 ***Influenza virus and quantification.*** The barcoded A/California/07/2009 (H1N1;  
358 H1N1pdm09) virus was propagated from low multiplicity of infection in MDCK cells (kindly  
359 provided by Dr. Daniel Perez, University of Georgia). Infectious virus concentrations were  
360 quantified on MDCK cells (kindly provided by Dr. Kanta Subbarao, World Health Organization)

361 using the tissue culture infectious dose 50 (TCID<sub>50</sub>) Spearman Kaber method, as previously  
362 described (56).

363 **Animal work.** Male ferrets, aged four to six months, were obtained from Triple F Farms  
364 (Sayre, Pennsylvania, USA). Prior to arrival, all ferrets were screened via hemagglutinin  
365 inhibition assay for antibodies against circulating influenza A and B viruses, as previously  
366 described (57).

367 All animal work was conducted in a biosafety level 2 at the University of Pittsburgh  
368 according to the guidelines of the Institutional Animal Care and Use Committee (approved  
369 protocol 22061230). Animals were sedated with isoflurane following approved methods for all  
370 nasal washing, oral swabbing, and blood draws.

371 Donor ferrets were inoculated intranasally with ~10<sup>6</sup> TCID<sub>50</sub> of barcoded H1N1pdm09,  
372 250 µL administered into each nostril. Oral swabs and nasal washes were taken for recipient  
373 ferrets on days 2, 3, 4, 5, 6, 8, and 10 post donor infection. Donor ferret oral swabs and nasal  
374 washes were collected on days 1, 2, 3, 5, and 7 post-infection. Blood draws were collected on  
375 days 0, 14, and 21 post donor infection to evaluate seroconversion of donors and recipients, and  
376 serological assays were performed as previously described (57). The neutralizing titer was  
377 defined as the inverse of the highest serum dilution needed to completely neutralize the  
378 infectivity of 10<sup>3.3</sup> TCID<sub>50</sub> of virus on MDCK cells.

379 **Close-range, play-based exposure.** The exposure space was comprised of vinyl flooring  
380 and a wire cage enclosure intended for use with large animals. The cage enclosure was ~74 cm  
381 tall and had a total footprint of 3.5 m<sup>2</sup> (Fig. 1). Food, water, and toys were placed in the  
382 enclosure. A remote-controlled robot was also deployed, which contained air samplers and  
383 sensors as described below under Environmental sample collection. A steel tent frame

384 surrounded the ferret enclosure, and during the low ventilation exposure, a fabric tent cover was  
385 attached to the frame and connected to the flooring material with Velcro to minimize air  
386 exchange. A large clear plastic viewing window was located on one side of the tent to allow for  
387 observation. Three GoPro cameras were placed on the tent frame to record ferret behavior and  
388 interactions during the exposure. Aranet4 sensors (SAF, Model TDSPC0H3) were distributed  
389 throughout the enclosure and recorded CO<sub>2</sub>, relative humidity, temperature, and partial pressure  
390 every minute. One Aranet4 sensor was kept outside of the enclosure as a measure of ambient  
391 CO<sub>2</sub> levels.

392 Four naïve recipient ferrets and one infected donor ferret (one day post-infection) were  
393 placed in the enclosure for four hours. After four hours of continuous exposure, all ferrets were  
394 removed and placed in individual housing for the next 10 days.

395 ***Measurement of air exchange rate.*** To establish the air exchange rate within the tent, the  
396 CO<sub>2</sub> decay method was used (58). Specifically, CO<sub>2</sub> levels in the tent were increased using dry  
397 ice and the atmosphere in the tent was well-mixed using a fan. Once CO<sub>2</sub> concentrations were  
398 sufficiently elevated above the background, the dry ice was removed and the fan was turned off.  
399 Aranet4 sensors in the tent recorded CO<sub>2</sub> every minute. During replicate 1, two sensors were  
400 distributed throughout the tent, and during replicate 2, four sensors were distributed throughout  
401 the tent. The average CO<sub>2</sub> concentration measured by all Aranets inside the tent was used for air  
402 exchange rate calculations. An Aranet4 sensor was also kept outside the tent as a measure of  
403 ambient CO<sub>2</sub>. The air exchange rate was calculated using CO<sub>2</sub> ratios with the following equation:

$$404 \quad Air \ exchange \ rate = \frac{-\ln \left( \frac{C_{end} - C_{ambient}}{C_{start} - C_{ambient}} \right)}{t_{end} - t_{start}}$$

405 Where  $C_{end}$  and  $C_{start}$  are the final and initial  $\text{CO}_2$  levels in the tent, respectively, and  $C_{ambient}$  is  
406 the background level of  $\text{CO}_2$  outside the tent.  $t_{start}$  and  $t_{end}$  were the times associated with the  
407 initial and final  $\text{CO}_2$  concentrations during the decay experiment. Two decay experiments were  
408 conducted, prior to each set of replicate exposures, and the average air exchange rate from these  
409 replicates was used.

410 Air exchange rate without the tent was determined using the mechanical ventilation data  
411 provided by the building during both experimental replicates. The following equation was used  
412 to determine air exchange:

$$413 \quad \text{Air exchange rate} = \frac{\text{Exhaust airflow}}{\text{Room volume}}$$

414 Where exhaust airflow is the rate at which the air is pulled mechanically from the room, in cubic  
415 feet per hour, and the room volume is the total volume of the space, in cubic feet. These values  
416 were provided by building facilities management. The exhaust airflow was  $\sim 1,770 \text{ m}^3\text{h}^{-1}$  for the  
417 room, which had a volume of  $76.5 \text{ m}^3$ , resulting in an air exchange rate of  $\sim 23 \text{ hr}^{-1}$  for the room.

418 ***Environmental sample collection.*** Surface samples were collected following each  
419 exposure experiment. Sterile foam-tip swabs were used (Puritan, Cat. No. 25-1506 1PF BT) to  
420 sample surfaces and subsequently placed in 1 mL collection medium, comprised of 0.5% filter-  
421 sterilized bovine serum albumin (Sigma-Aldrich, Cat. No. A3294) in 1X PBS (Sigma-Aldrich,  
422 Cat. No. P4417). All swabs were pre-wetted in collection medium. Flat surfaces were swabbed  
423 using a 10 cm x 10 cm stencil, and toys, food containers, and water dispensers were swabbed as  
424 completely as possible. Three pre-exposure surface samples were taken before each experiment  
425 as negative controls. Following collection, surface swab samples were aliquoted for titering and  
426 RNA extraction and stored at  $-80^\circ\text{C}$  until downstream analysis.

427 NIOSH multi-stage bioaerosol cyclone samplers (Tisch Environmental, Model TE-  
428 BC251), a Liquid Spot Sampler aerosol particle collector (Aerosol Devices, Series 110B), and a  
429 gelatin cassette were used to collect air samples during each exposure period. NIOSH bioaerosol  
430 cyclone samplers were cleaned with isopropanol and milliQ prior to each use. Particles  $> 4 \mu\text{m}$ , 1  
431  $- 4 \mu\text{m}$ , and  $< 1 \mu\text{m}$  were collected into a sterile 15 mL tube (Falcon, Cat. No. 352096), sterile  
432 1.5 mL tube (Fisherbrand, Cat. No. 02-681-373), and 37 mm polytetrafluoroethylene filter  
433 (Millipore, Cat. No. FSLW03700) with backing filter, respectively. Disposable 37 mm sterile  
434 plastic cassettes (Pall, Cat. No. 4339-N) were used to collect air on 37 mm sterile gelatin filters  
435 (3  $\mu\text{m}$  pore size; Sartorius, Cat. No. 12602-37-ALK) containing a backing filter to ensure the  
436 gelatin filter remained intact during sampling. Samplers were connected to GilAir-5 air sampling  
437 pumps (Sensidyne, Part 800883-171) with flow rates of 3.5 L/min and 1.5 L/min for the NIOSH  
438 bioaerosol cyclone samplers and gelatin cassette, respectively. Two NIOSH bioaerosol cyclone  
439 samplers and one gelatin cassette were contained in the robot housing, while the remaining  
440 NIOSH bioaerosol cyclone samplers were placed at various locations around the enclosure (Fig.  
441 2). The Spot sampler collected air at  $\sim 1.4 \text{ L/min}$  with the following settings: 5°C for the  
442 conditioner, 40°C for the initiator, 18°C for the moderator, and 27°C for the nozzle. Antistatic  
443 silicone tubing (McMaster Carr, Part 1909T39) was used to take in air at ferret height (i.e., 6") in  
444 the close-contact exposure. All samplers ran during the entire exposure period. Baseline air  
445 sampling was conducted three to four days prior to each round of experiments. Four of five  
446 NIOSH bioaerosol cyclone samplers were processed by adding 500  $\mu\text{L}$  MagMax Lysis/Binding  
447 Solution Concentrate (ThermoFisher, Cat. No. AM8500) to each air collection fraction, while the  
448 fractions of the fifth NIOSH bioaerosol cyclone sampler were each processed using 1 mL  
449 collection medium to assess whether infectious virus could be recovered from NIOSH bioaerosol

450 cyclone samplers. Samples were each vortexed vigorously for one minute, centrifuged briefly,  
451 and placed in 1.5 mL microcentrifuge tubes. Gelatin filters were removed from cassettes, placed  
452 in 15 mL centrifuge tubes, and dissolved by incubating filters with 1 mL collection medium at  
453 37°C for five minutes, with intermittent vortexing. All samples were stored at -80°C until  
454 downstream processing.

455 ***Direct air sampling of donor ferrets.*** The Spot sampler was used to collect air directly  
456 from infected donors on days 1, 2, and 3 post-infection. The collection period was 15 minutes  
457 long, resulting in ~ 21 L of total air sampled. A 7L induction chamber (Vet Equip, Cat. No.  
458 941448) with an inlet and outlet was used to contain the ferret during sampling. Antistatic tubing  
459 was connected from the box outlet to the sampler inlet. Makeup air came from the box inlet.  
460 Aerosols were collected into 400  $\mu$ L collection medium, and following sample collection, the  
461 total sample volume was increased to 700  $\mu$ L. To ensure no carry-over of virus, the wick was  
462 cleaned between samples by first flushing with 6 mL of isopropanol and subsequently flushing  
463 with 18 mL of milliQ water. Clean tubing was used for each sample, and collection vials were  
464 cleaned thoroughly with ethanol.

465 ***Infectious virus quantification of environmental samples.*** Infectious influenza virus  
466 concentrations in surface samples and a subset of air samples were determined on Madin-Darby  
467 Canine Kidney Cells (MDCK; kindly provided by Dr. Kanta Subbarao) via the Spearman Kaber  
468 TCID<sub>50</sub> assay, as previously described (56).

469 ***Viral RNA quantification of environmental samples.*** 200  $\mu$ L of each surface sample was  
470 extracted using the PureLink Viral RNA/DNA Mini Kit (ThermoFisher, Cat. No. 12280050)  
471 according to the standard protocol, with a final elution volume of 50  $\mu$ L. Air samples were  
472 extracted using the QIAamp Viral RNA Mini Kit (QIAGEN, Cat. No. 52904) as specified. 140

473       $\mu$ L of Spot samples and gelatin cassette samples were extracted, while 500  $\mu$ L of NIOSH  
474      samples were extracted. All air samples were eluted in 60  $\mu$ L nuclease-free water. Extracts were  
475      stored at -80°C until RNA quantification.

476              Viral RNA levels in all extracted samples were established via RT-qPCR of the matrix  
477      gene, using a previously published set of USDA primers and probe with slight modifications  
478      (Forward: 5'-AGATGAGTCTTCTAACCGAGGTCG-3', Reverse: 5'-  
479      GCAAAGACACTTCCAGTCTCTG-3', Probe: 5'- FAM-TCAGGCCCTCAAAGCCGA-  
480      BHQ-3') (59). All reactions were conducted using the iTaq Universal Probes One-Step RT-  
481      qPCR Kit (BioRad, Cat. No. 1725141) on a CFX Connect Real-Time PCR Detection System  
482      (BioRad, Cat. No. 1855201) with the following thermocycling conditions: reverse transcription  
483      at 50°C for 10 minutes, initial denaturation at 95°C for 2 min, followed by 40 cycles of  
484      denaturation and combined annealing/extension at 95°C and 60°C for 10 sec and 20 sec,  
485      respectively. In vitro transcribed RNA of the full-length matrix gene was used as the assay  
486      standard, and the limit of detection was established as previously described (60). Samples were  
487      run in technical duplicates, and any samples that had replicates > 1 Ct apart or had no Ct value  
488      for one of two replicates were re-run. If re-runs yielded replicates > 1 Ct apart or had no Ct value  
489      for one or both replicates, the viral RNA concentration was defined as below the limit of  
490      detection. No template controls were run on each plate.

491              ***Sample processing for next-generation sequencing.*** Viral RNA extraction from nasal  
492      washes of infected ferrets was done using the Quick-RNA Viral 96 Kit (Zymo, Cat. No. R1040)  
493      using 160  $\mu$ L sample volume. This was followed by a one-step RT-PCR reaction using the  
494      SuperScript III One-Step RT-PCR System with Platinum Taq High Fidelity DNA Polymerase  
495      (ThermoFisher, Cat. No. 12574035) and primers targeting the barcoded region (Forward 5' -

496 TCGTCGGCAGCGTCAGATGTGTATAAGAGACAGACCTTCTTCTGACTCAAGGG – 3’;

497 Reverse 5’ –

498 GTCTCGTGGGCTCGGAGATGTGTATAAGAGACAGCAAGCGACTGACTCAAATCTG

499 A – 3’). The first 33 nucleotides in the primer correspond to adapter sequences for sequencing in

500 the Illumina MiSeq platform. Following amplicon generation, samples were purified using

501 AMPure XP Beads (Beckman Coulter, Cat. No. A63881) with a concentration suitable for the

502 amplicon size (250 bp). Next, DNA quantification was done using the Qubit dsDNA

503 quantification kit (ThermoFisher, Cat. No. Q32851). Samples were submitted to Emory

504 Integrated Genomics Core where indexing (Nextera XT – Illumina), bead cleaning, quality

505 control via bioanalyzer, pooling, and Illumina MiSeq sequencing were completed.

506 ***Amplicon sequencing analysis.*** Barcode sequences were analyzed using BarcodeID, a

507 software developed in the Lowen laboratory. BarcodeID processes the raw sequences using the

508 BBtools suite (61), before screening reads to ensure that each has the expected base at barcode

509 and non-barcode sites, and that these bases are high quality (Phred values  $\geq 30$  and  $\geq 25$ , for

510 barcode and non-barcode sites, respectively). Importantly, BarcodeID records the frequency of

511 high-quality bases that don’t match the expected amplicon and barcode sequence, which is used

512 to identify *de novo* mutations that are driving barcode dynamics. No such *de novo* mutations

513 were detected in the present dataset. BarcodeID is available on GitHub at

514 <https://github.com/Lowen-Lab/BarcodeID>.

515

## Data, Materials, and Software Availability

All data are available on FigShare upon publication. BarcodeID code is available on Github at <https://github.com/Lowen-Lab/BarcodeID>.

## Acknowledgments

We thank the MITIGATE FLU team, the Lakdawala Laboratory, and Rachel Duron for critical review and feedback. We thank Milan Shah (Conestoga High School student, Chesterbrook PA) for construction of ERINE. This work was funded by FluLab. Sequencing work was supported by the Emory Integrated Genomics Core Facility (RRID:SCR\_023529).

## References

1. C. E. Troeger, *et al.*, Mortality, morbidity, and hospitalisations due to influenza lower respiratory tract infections, 2017: an analysis for the Global Burden of Disease Study 2017. *Lancet Respir Med* **7**, 69–89 (2019).
2. G. Brankston, L. Gitterman, Z. Hirji, C. Lemieux, M. Gardam, Transmission of influenza A in human beings. *Lancet Infect Dis* **7**, 257–265 (2007).
3. N. H. L. Leung, Transmissibility and transmission of respiratory viruses. *Nat Rev Microbiol* **19**, 528–545 (2021).
4. B. Killingley, J. Nguyen-Van-Tam, Routes of influenza transmission. *Influenza Other Respir Viruses* **7**, 42–51 (2013).
5. B. J. Cowling, *et al.*, Aerosol transmission is an important mode of influenza A virus spread. *Nat Commun* **4**, 1935 (2013).
6. L. C. Marr, J. W. Tang, A Paradigm Shift to Align Transmission Routes With Mechanisms. *Clinical Infectious Diseases* **73**, 1747–1749 (2021).
7. J. P. Collins, A. L. Shane, Infections Associated With Group Childcare. *Principles and Practice of Pediatric Infectious Diseases*, 25-32.e3 (2018).
8. I. R. A. M. LONGINI JR., J. S. KOOPMAN, A. S. MONTO, J. P. FOX, ESTIMATING HOUSEHOLD AND COMMUNITY TRANSMISSION PARAMETERS FOR INFLUENZA. *Am J Epidemiol* **115**, 736–751 (1982).
9. T. K. Tsang, L. L. H. Lau, S. Cauchemez, B. J. Cowling, Household Transmission of Influenza Virus. *Trends Microbiol* **24**, 123–133 (2016).
10. D. Bell, *et al.*, Non-pharmaceutical interventions for pandemic influenza, international measures. *Emerg Infect Dis* **12**, 81–87 (2006).
11. C. R. MacIntyre, *et al.*, A cluster randomized clinical trial comparing fit-tested and non-fit-tested N95 respirators to medical masks to prevent

respiratory virus infection in health care workers. *Influenza Other Respir Viruses* **5**, 170–179 (2011).

- 12. J. Xiao, *et al.*, Nonpharmaceutical Measures for Pandemic Influenza in Nonhealthcare Settings—Personal Protective and Environmental Measures. *Emerging Infectious Disease journal* **26**, 967 (2020).
- 13. P. K. Ram, *et al.*, Impact of Intensive Handwashing Promotion on Secondary Household Influenza-Like Illness in Rural Bangladesh: Findings from a Randomized Controlled Trial. *PLoS One* **10**, e0125200–e0125200 (2015).
- 14. T. Suess, *et al.*, The role of facemasks and hand hygiene in the prevention of influenza transmission in households: results from a cluster randomised trial; Berlin, Germany, 2009–2011. *BMC Infect Dis* **12**, 26 (2012).
- 15. A. S. Azman, *et al.*, Household transmission of influenza A and B in a school-based study of non-pharmaceutical interventions. *Epidemics* **5**, 181–186 (2013).
- 16. S. Stebbins, *et al.*, Reduction in the incidence of influenza A but not influenza B associated with use of hand sanitizer and cough hygiene in schools: a randomized controlled trial. *Pediatr Infect Dis J* **30**, 921–926 (2011).
- 17. M. Talaat, *et al.*, Effects of hand hygiene campaigns on incidence of laboratory-confirmed influenza and absenteeism in schoolchildren, Cairo, Egypt. *Emerg Infect Dis* **17**, 619–625 (2011).
- 18. A. E. Aiello, *et al.*, Facemasks, Hand Hygiene, and Influenza among Young Adults: A Randomized Intervention Trial. *PLoS One* **7**, e29744- (2012).
- 19. C. R. MacIntyre, *et al.*, The efficacy of medical masks and respirators against respiratory infection in healthcare workers. *Influenza Other Respir Viruses* **11**, 511–517 (2017).
- 20. B. Killingley, *et al.*, Potential role of human challenge studies for investigation of influenza transmission. *Lancet Infect Dis* **11**, 879–886 (2011).
- 21. J. S. Nguyen-Van-Tam, *et al.*, Minimal transmission in an influenza A (H3N2) human challenge-transmission model within a controlled exposure environment. *PLoS Pathog* **16**, e1008704 (2020).
- 22. B. Killingley, *et al.*, Use of a Human Influenza Challenge Model to Assess Person-to-Person Transmission: Proof-of-Concept Study. *J Infect Dis* **205**, 35–43 (2012).
- 23. V. Le Sage, A. C. Lowen, S. S. Lakdawala, Block the Spread: Barriers to Transmission of Influenza Viruses. *Annu Rev Virol* (2023) <https://doi.org/10.1146/annurev-virology-111821-115447>.
- 24. T. R. Maines, *et al.*, Lack of transmission of H5N1 avian–human reassortant influenza viruses in a ferret model. *Proceedings of the National Academy of Sciences* **103**, 12121–12126 (2006).
- 25. M. L. Herlocher, *et al.*, Ferrets as a Transmission Model for Influenza: Sequence Changes in HA1 of Type A (H3N2) Virus. *J Infect Dis* **184**, 542–546 (2001).

26. F. Koster, *et al.*, Exhaled Aerosol Transmission of Pandemic and Seasonal H1N1 Influenza Viruses in the Ferret. *PLoS One* **7**, e33118- (2012).
27. T. C. Sutton, *et al.*, Sequential Transmission of Influenza Viruses in Ferrets Does Not Enhance Infectivity and Does Not Predict Transmissibility in Humans. *mbio* **13**, e02540-22 (2022).
28. M. Imai, *et al.*, Experimental adaptation of an influenza H5 HA confers respiratory droplet transmission to a reassortant H5 HA/H1N1 virus in ferrets. *Nature* **486**, 420–428 (2012).
29. J. A. Belser, *et al.*, Ferrets as Models for Influenza Virus Transmission Studies and Pandemic Risk Assessments. *Emerg Infect Dis* **24**, 965–971 (2018).
30. E. M. Sorrell, H. Wan, Y. Araya, H. Song, D. R. Perez, Minimal molecular constraints for respiratory droplet transmission of an avian–human H9N2 influenza A virus. *Proceedings of the National Academy of Sciences* **106**, 7565–7570 (2009).
31. Q. Zhang, *et al.*, H7N9 Influenza Viruses Are Transmissible in Ferrets by Respiratory Droplet. *Science* (1979) **341**, 410–414 (2013).
32. V. J. Munster, *et al.*, Pathogenesis and Transmission of Swine-Origin 2009 A(H1N1) Influenza Virus in Ferrets. *Science* (1979) **325**, 481–483 (2009).
33. V. Le Sage, *et al.*, Pre-existing heterosubtypic immunity provides a barrier to airborne transmission of influenza viruses. *PLoS Pathog* **17**, e1009273 (2021).
34. K. L. Roberts, H. Shelton, P. Stilwell, W. S. Barclay, Transmission of a 2009 H1N1 Pandemic Influenza Virus Occurs before Fever Is Detected, in the Ferret Model. *PLoS One* **7**, e43303 (2012).
35. World Health Organization, “Non-pharmaceutical public health measures for mitigating the risk and impact of epidemic and pandemic influenza” (2019).
36. Centers for Disease Control and Prevention, Nonpharmaceutical Interventions (NPIs) (2022) (September 10, 2023).
37. M. R. MOSER, *et al.*, AN OUTBREAK OF INFLUENZA ABOARD A COMMERCIAL AIRLINER. *Am J Epidemiol* **110**, 1–6 (1979).
38. X. Gao, Y. Li, G. M. Leung, Ventilation Control of Indoor Transmission of Airborne Diseases in an Urban Community. *Indoor and Built Environment* **18**, 205–218 (2009).
39. L. Liu, Y. Li, P. V Nielsen, J. Wei, R. L. Jensen, Short-range airborne transmission of expiratory droplets between two people. *Indoor Air* **27**, 452–462 (2017).
40. X. Gao, J. Wei, B. J. Cowling, Y. Li, Potential impact of a ventilation intervention for influenza in the context of a dense indoor contact network in Hong Kong. *Science of The Total Environment* **569–570**, 373–381 (2016).
41. S.-C. Chen, C.-M. Liao, Modelling control measures to reduce the impact of pandemic influenza among schoolchildren. *Epidemiol Infect* **136**, 1035–1045 (2008).

42. A. Varble, *et al.*, Influenza A Virus Transmission Bottlenecks Are Defined by Infection Route and Recipient Host. *Cell Host Microbe* **16**, 691–700 (2014).
43. R. Frise, *et al.*, Contact transmission of influenza virus between ferrets imposes a looser bottleneck than respiratory droplet transmission allowing propagation of antiviral resistance. *Sci Rep* **6**, 29793 (2016).
44. P. G. FISHER, FERRET BEHAVIOR. *Exotic Pet Behavior*, 163–205 (2006).
45. B. Kolarik, *et al.*, Ventilation in day care centers and sick leave among nursery children. *Indoor Air* **26**, 157–167 (2016).
46. S. Batterman, *et al.*, Ventilation rates in recently constructed U.S. school classrooms. *Indoor Air* **27**, 880–890 (2017).
47. Centers for Disease Control and Prevention, Guidelines for Environmental Infection Control in Health-Care Facilities (2003).
48. J. A. Belser, *et al.*, Robustness of the Ferret Model for Influenza Risk Assessment Studies: a Cross-Laboratory Exercise. *mBio* **13**, e01174-22 (2022).
49. S. Asadi, *et al.*, Influenza transmission in the guinea pig model is insensitive to the ventilation airflow speed: Evidence for the role of aerosolized fomites. *Phys Rev Fluids* **8**, 40502 (2023).
50. J. S. Nguyen-Van-Tam, *et al.*, Minimal transmission in an influenza A (H3N2) human challenge-transmission model within a controlled exposure environment. *PLoS Pathog* **16**, e1008704 (2020).
51. R. and A.-C. E. American Society of Heating, ASHRAE Standard 241, Control of Infectious Aerosols (2023).
52. B. Killingley, *et al.*, The environmental deposition of influenza virus from patients infected with influenza A(H1N1)pdm09: Implications for infection prevention and control. *J Infect Public Health* **9**, 278–288 (2016).
53. A. Chamseddine, *et al.*, Detection of influenza virus in air samples of patient rooms. *Journal of Hospital Infection* **108**, 33–42 (2021).
54. K. E. Holmes, *et al.*, Viral expansion after transfer is a primary driver of influenza A virus transmission bottlenecks. *bioRxiv*, 2023.11.19.567585 (2023).
55. E. Hoffmann, G. Neumann, G. Hobom, R. G. Webster, Y. Kawaoka, “Ambisense” Approach for the Generation of Influenza A Virus: vRNA and mRNA Synthesis from One Template. *Virology* **267**, 310–317 (2000).
56. M. A. Ramakrishnan, Determination of 50% endpoint titer using a simple formula. *World J Virol* **5**, 85–86 (2016).
57. V. Le Sage, *et al.*, Pre-existing heterosubtypic immunity provides a barrier to airborne transmission of influenza viruses. *PLoS Pathog* **17**, e1009273 (2021).
58. J. Allen, J. Spengler, E. Jones, J. Cedeno-Laurent, “5-step guide to checking ventilation rates in classrooms” (2020).
59. E. Spackman, *et al.*, Development of a Real-Time Reverse Transcriptase PCR Assay for Type A Influenza Virus and the Avian H5 and H7 Hemagglutinin Subtypes. *J Clin Microbiol* **40**, 3256–3260 (2002).

60. L. Hougs, *et al.*, “Verification of analytical methods for GMO testing when implementing interlaboratory validated methods” (2017).
61. B. Bushnell, BBMap: A Fast, Accurate, Splice-Aware Aligner. (2014).